Color compensation in anomalous trichromats assessed with fMRI

Katherine E.M. Tregillus[1,2], Zoey J. Isherwood[1], John E. Vanston[1], Stephen A. Engel[2], Donald I.A. MacLeod[3], Ichiro Kuriki[4], Michael A. Webster[1]

1. Department of Psychology, University of Nevada, Reno
2. Department of Psychology, University of Minnesota, Twin Cities
3. Department of Psychology, University of California, San Diego
4. Research Institute for Electrical Communication, Tohoku University, Sendai

Abstract

Anomalous trichromacy is a common form of congenital color-deficiency resulting from a genetic alteration in the photopigments of the eye's light receptors. The changes reduce sensitivity to reddish-greenish hues, yet previous work suggests that these observers may experience the world to be more colorful than their altered receptor sensitivities would predict, potentially indicating an amplification of post-receptoral signals. However, past evidence suggesting such a gain adjustment rests on subjective measures of color appearance or salience. We directly tested for neural amplification by using fMRI to measure cortical responses in color-anomalous and normal control observers. Color contrast response functions were measured in two experiments with different tasks to control for attentional factors. Both experiments showed a predictable reduction in chromatic responses for anomalous trichromats in primary visual cortex. However, in later areas V2v and V3v, chromatic responses in the two groups were indistinguishable. Our results provide direct evidence for neural plasticity that compensates for the deficiency in the initial receptor color signals and suggest that the site of this compensation is in early visual cortex.

Introduction

Typical color perception in humans is trichromatic, beginning with responses to light from three types of cone photoreceptors, known as long-, medium-, and short-wave receptors (L, M, and S) according to the wavelengths they are most sensitive to. A second stage of processing compares signals from the cones; for example the L and M cone responses are subtracted from each other in post-receptoral cells that receive opposing inputs (excitation or inhibition) from them. However, in common inherited color deficiencies the L or M cone gene is absent or altered [1-3], leading to a loss of one receptor type (dichromacy), or to a shift in wavelength sensitivity of the affected cone so that it is more similar to the normal M or L cone (anomalous trichromacy). The latter results in a smaller difference in the L vs M signal, and produces weaker sensitivity to reddish-greenish colors [4-7]. As an X-linked recessive trait, this class of color deficiencies affect 6-8% of people with XY chromosomes, but is relatively rare in those with XX (<1%).

Color deficiencies are often modeled as a reduced form of normal trichromacy, in which visual processing is the same except for an initial alteration in the photopigments. This reduction model

accounts well for poorer color detection and discrimination thresholds in color deficient observers, and has played a critical role in estimating the cone spectral sensitivities [8, 9]. It also is the basis for most simulations of color deficiencies [10-12]. However, this reduction model does not consider potential plasticity in visual coding, which could in principle compensate for a loss in sensitivity by amplifying the post-receptoral difference signals. In anomalous trichromats, the weakened L vs M signal could be restored by gain changes within color-opponent mechanisms, analogous to turning up the contrast on a monitor [13, 14]. Testing for such amplification provides an ideal natural model for studying the limits of long-term compensation in the visual system.

Yet despite this theoretical importance, whether and how color compensation occurs in anomalous trichromacy remains poorly understood. The thresholds for discriminating color differences are well predicted by the cone sensitivities, and are the basis for common color screening tests [15-20]. However above threshold the results are more mixed, with some tasks showing the expected losses and others providing evidence for compensation (for review see [21]). The tasks indicating compensation tend to involve judging the similarity or size or salience of color differences [22-24], and thus could potentially reflect conceptual rather than perceptual adaptations.

There have been few direct tests of compensation by measuring neural activity [25], and to our knowledge none using functional MRI to assess color processing in anomalous trichromats, a technique that has been shown to be an effective measure of color and contrast coding throughout cortex [26-31] [32-35]. Primary visual cortex appears to show some plasticity with respect to color over both the long [36] and short term [37], the latter consistent with numerous psychophysical and physiological studies [38, 39]. Thus, if amplification occurs in the neural responses to color for anomalous observers, then early visual cortex is a likely candidate site.

Results

Detection Thresholds

As expected due to their shifted cone responses, anomalous trichromat observers showed dramatically higher thresholds for detecting stimuli defined by L vs M cone differences. Thresholds were collected for 5 out of the 7 anomalous trichromat (AT) observers, and 6 of the 7 controls (CN) (Figure 1).

On average L vs M thresholds were 7.3 times higher for AT than control participants (AT mean = 9.39, AT SD = 1.81, CN mean = 1.29, CN SD = 0.25, $t(9) = 10.976$, $P<0.001$), while thresholds for detecting S vs LM stimuli, which should be relatively unaffected by the color deficiency, did not significantly differ (S vs LM color axis; AT mean = 1.77, AT SD = 0.35, CN mean = 1.71, CN SD = 0.57, $t(9) = 0.221$, $P = 0.830$).

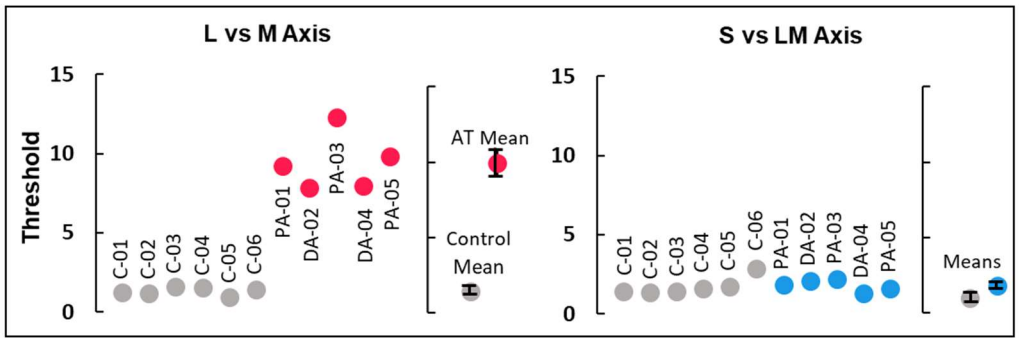

Figure 1. Chromatic contrast detection thresholds for the two chromatic axes, represented in nominal multiples of threshold where thresholds for observers with no color deficits should be at about 1. Settings are shown for each individual observer and for the mean of the control (gray) or anomalous (red or blue) participants. Error bars represent one standard error of the mean.

Experiment 1: Simple Fixation Task

We conducted two fMRI experiments to assess neural responses to chromatic contrast in the AT and CN observers. In the first, data were collected from a total of 10 participants (5 CN, 2 deuteranomalous, and 3 protanomalous AT), and stimuli consisted of reversing radial sinewave gratings along the 2 chromatic axes presented at 4 contrast levels (Figure 2a). Participants monitored the fixation point for occasional changes (from black to white) to ensure they were attending to the display. fMRI responses to the gratings arose most strongly in early visual areas, and the amount of activation was similar across groups, with greater chromatic responses in the ventral portions of V2 and V3 than in other regions, consistent with previous work [40]. Accordingly, we used the ventral portions of V2 and V3 in all analyses (Figure 2b, 3).

The fMRI data showed reduced responses to L vs M stimuli for AT observers compared to normals in V1, but strikingly this reduction disappeared in V2 and V3, consistent with amplification in these later areas (Figure 2). The statistical reliability of this pattern was assessed with a 2 x (3 x 2 x 4) mixed ANOVA using the β weights calculated from the GLM analysis of the fMRI data. The between subject factor was *Observer Type* (CN, AT), and the three within subject factors were *Visual Area* (V1, V2v, V3v), *Color Axis* (L vs M, S vs LM), and *Contrast* (10, 20, 40, 80 in nominal threshold units). Post-hoc pairwise comparisons were performed for the L vs M data in each ROI. Critically, there was a significant difference between anomalous trichromats and color-normals ($t(8) = 2.38$, $p = 0.04$) in the L vs M response in V1, but not in V2v ($t(8) = 1.09$, $p = 0.31$) or V3v ($t(8) = 0.56$, $p = 0.59$). In comparison AT and CN responses were relatively equal in all three areas for S vs LM contrast, where amplification was not predicted. This overall pattern was visible in the ANOVA as a highly significant interaction between Group, Visual Area, and Color Axis ($F_{1.449,14.491} = 5.909$, $p = 0.020$, $\eta_p^2 = 0.450$). See SI Table 1 for full ANOVA results.

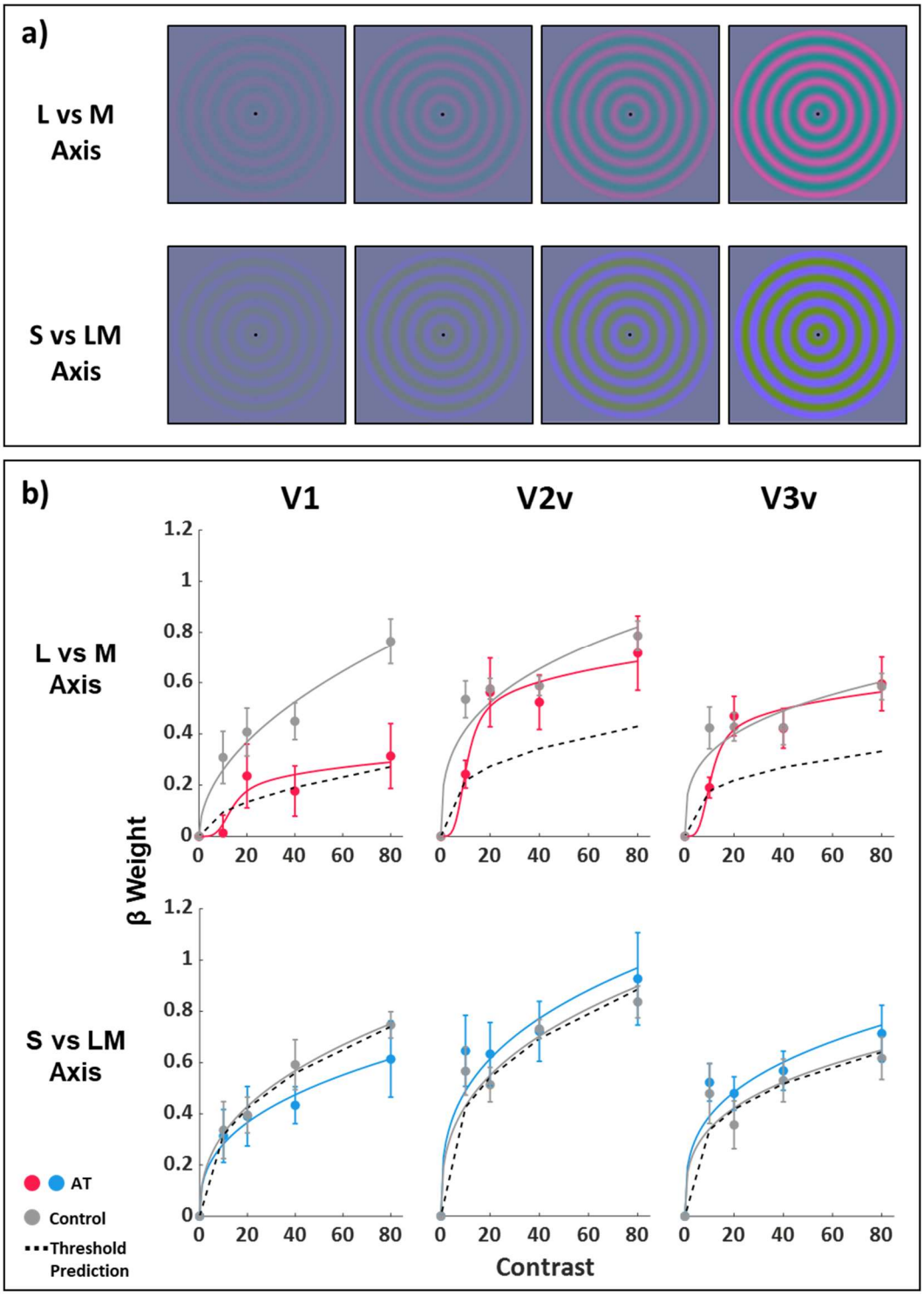

Figure 2. Results from Experiment 1. a) Illustration of the 2 color axes and 4 contrast levels used for both experiments. b) Points are β weights from Exp. 1, representing the estimated amplitude of the fMRI response during the simple fixation task. The top row are responses to the L vs M stimuli, and the bottom row are responses to the S vs LM stimuli. Columns are the three regions-of-interest: V1 (left), V2v (center), and V3v (right). The solid red and blue lines are model contrast response functions (CRFs) fitted to the data. The black dashed lines are response predictions for the AT group using the reduction model (see main text). Error bars are standard error of the mean.

Experiment 2: High-Attentional Fixation

A second experiment was designed to replicate our results using a more demanding attentional task. Attention and task can strongly modulate fMRI responses and alter the relationship between response amplitude and stimulus contrast [41, 42], as well as the representation of color, especially in later visual areas [33]. In this experiment we used a highly-demanding fixation task to further isolate "bottom-up" processing to the unattended color patterns. As in past work, observers monitored a stream of black and white numbers at fixation for specific feature conjunctions (e.g. a white 3) [43]. Measurements were collected for 5 AT and 7 CN observers.

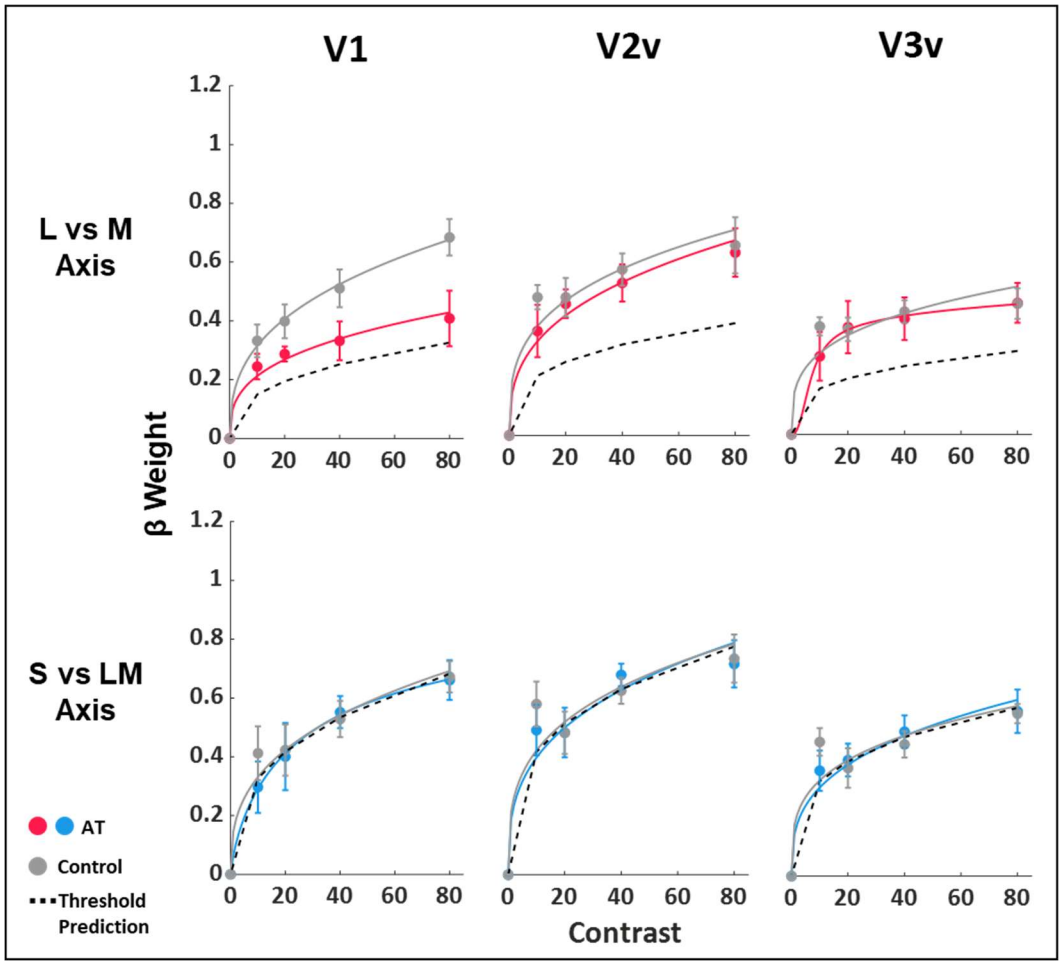

Figure 3. Results from Experiment 2, high-attention fixation task for the L vs M axis. Plotting conventions are as in Figure 2.

The fMRI data revealed a very similar pattern to that observed in Experiment 1, again supporting amplification – with weaker L vs M responses in V1 for AT observers, but not in later regions (Figure 3, V1: $t(10) = 2.73$, $p = 0.02$, V2v: $t(10) = 0.85$, $p = 0.41$, V3v: $t(10) = 0.44$, $p = 0.66$), see SI table 2 for full ANOVA results. The closeness of the two curves suggests that amplification almost completely compensated for receptoral differences by bringing AT cortical responses to

CN levels. As in Experiment 1, there were no reliable differences between the ATs and CNs in cortical responses to S vs LM contrasts.

5 CNs and 3 ATs participated in both Experiments 1 and 2. We used their data to compare the two attention tasks. (See SI Figure 1). Overall, AT participants showed slightly lower activation in general during the simple fixation task, but this difference was not significant and only appeared in area V1. We also found no significant effects of attention task ($F_{1,6.000} = 3.736$, $p = 0.101$, $\eta_p^2 = 0.384$). (See SI Table 3 for full ANOVA.)

Testing for Amplification by Modeling Contrast Response

To quantify post-receptoral gain in the chromatic signal, we compared cortical responses to an implementation of the reduction model. As a first step, we quantified how responses varied with contrast, by fitting to the data a standard contrast response function (CRF) [44]:

$$R(c) = R_{max} * \frac{c^{(p+q)}}{\left(c^q + c_{50}^q\right)}$$

where R is the measured BOLD response, c is the stimulus contrast, and p and q are exponents controlling the function's shape. Rmax, c50, p, and q were all allowed to vary. The fitted functions are shown as the solid lines in Figures 2b and 3, with control observers in gray, and AT observers in red and blue, and these fitted functions accounted for the data well.

We next compared responses of AT observers to predictions of the reduction model, which assumes that all differences between groups are due to receptoral differences (and that no amplification occurs). Detection thresholds have been shown to vary inversely with the separation between the L and M cone sensitivities, so that an observer whose threshold is, for example, 5 times higher than normal would have an L and M peak separation that is 5 times smaller and thus proportional to AT observers' threshold-level deficit [22]. The reduction model predicts that L and M peak separation also scales the L vs M differences above threshold, such that the CRF for anomalous trichromats should be equal to the CRF for control participants except for a rescaling of L vs M stimulus strength (contrast, c) by the ratio of normal to anomalous thresholds. The model predictions are shown as the black dashed line in Figures 2b and 3., and they approximate the weaker BOLD responses observed in V1 but clearly fall below the responses in V2v and V3v. (See SI Figure 2 for individual data and fits.), suggestive of amplification in the AT observers.

To quantify the amount of amplification, we instead scaled the stimulus contrast (c) to fit each AT observer's individual CRF, with other parameters held constant, and compared this to the contrast scaling predicted by the reduction model (i.e. scaled by their thresholds). A ratio of 1 would indicate that the AT's CRF was consistent with the reduction model, while values greater than 1 would indicate compensation. The resulting ratios again showed clear evidence for amplification. Mean values were 2.94 (sd = 2.81) for V1, 6.39 (sd = 5.21) for V2v, and 7.82 (sd = 5.76) for V3v. For Experiment 2, where we had threshold measures for all 5 AT observers, we compared this scaling factor to 1 (the reduction model prediction), and it was reliably above 1 in V2v ($t(4) = 5.12$,

$p = 0.007$) and in V3v ($t(4) = 4.265$, $p = 0.01$), but not in V1 ($t(4) = 1.42$, $p = 0.23$). We also performed a repeated measures ANOVA on the scaling factors and found a significant effect of ROI, ($F(2) = 4.977$, $p = 0.04$).

Discussion

Our results point to strong compensation for color losses in anomalous trichromacy through amplification of cortical responses to chromatic contrast. This in turn suggests that the greater than expected responses to colors observed behaviorally [22-24] may reflect actual gain changes in early cortical processing. Both the neural and behavioral evidence are not inconsistent with the profound sensitivity losses in color-anomalous observers in threshold discrimination for color, since these thresholds are limited by noise, which may also be amplified by the gain change [13, 14, 45]. The suprathreshold compensation for color contrast may be similar to effects observed for spatial contrast, where thresholds depend strongly on spatial frequency (pattern size) yet once above threshold perceived contrast is independent of frequency [46]. In this regard it is notable that less compensation is evident at the lowest contrast we tested (10) which was near the mean threshold for the anomalous observers.

Our results also point to an early but not initial stage of cortical coding as the site of the contrast amplification. Both experiments showed that the L vs M responses were consistent with the reduction model in V1 but were indistinguishable from color-normals in V2v and V3v. The fact that this pattern persisted under the attentionally demanding task of Experiment 2 suggests top-down modulation is not responsible for the neural gain occurring between V1 and V2v. We cannot rule out some amplification within V1, if for example the BOLD responses are disproportionately driven by cells in input layers or other neurons prior to compensation. Future studies examining laminar projections from V1 to V2 (for review see [47]) may be able to resolve this issue. However our findings do imply that there is relatively little compensation prior to V1. This conclusion is also consistent with a recent study using visual evoked potentials which found evidence for color compensation but only when the stimuli were viewed binocularly [25], implying a cortical site since signals from the two eyes first converge in V1.

The emergence of compensation in the cortex would mean that the retina and LGN remain in a weakened, unadjusted state for processing the L vs M signals. While there are increasing signs of short-term plasticity, specifically contrast adaptation, at these early stages [48-50], contrast adaptation is known to be substantially stronger in the visual cortex [51], especially within the parvocellular pathway along which the L vs M signals are carried [48, 52]. Given the plasticity of V1, it is not clear why a long-term adjustment for chromatic contrast would first emerge in V2. Chromatic processing is known to undergo a series of transformations along the ventral stream, though the function of different representations remains uncertain [32, 53-55].

The adjustments we measured could potentially represent a very long-term form of visual plasticity, though we cannot rule out a process that acts more rapidly. Color vision adjusts to changes in the environment or observer over widely varying timescales [56], and compensation for the color losses could similarly involve multiple timescales and processes. For example a recent study found that color percepts in anomalous observers could be enhanced after just a few days wearing glasses that increased the L vs M contrasts [57]. One potential mechanism that could account for the compensatory adjustments we observed is sensory adaptation, in which neural signals adjust to the average and range of the ambient stimulation [58]. If the contrast is too low, then a neuron may increase its sensitivity so that the range of outputs is maintained [59, 60]. Most studies of adaptation have focused on very short-term aftereffects and on sensitivity losses rather than gains. However, exposures to contrast losses as brief as a few hours have been found to lead to compensatory enhancements of contrast sensitivity [61-63]. Our study is a natural color analog of adapting to a contrast reduction but measured over a lifetime of exposure. However, this analogy raises the puzzle of why responses in V1 were not adjusted given profound adaptation at this level [64, 65].

The results of the present studies are relevant not only to color but to understanding adaptation and neural calibration more generally, for the patterns and mechanisms of plasticity appear to be very similar across sensory levels and modalities [39]. Our results suggest that the nervous system can, at least in some cases, almost completely compensate for aberrant initial coding of stimuli. How and under what circumstances such compensation can occur has important implications for treatment of visual disorders, as well as for the increasing prospects of gene therapy for color deficiencies [66].

Methods

Anomaloscope

The color vision of all participants was assessed using standard color screening techniques, including Rayleigh matching using a Heidelbert-Multi-Color Anomaloskop (OCULUS, Inc., Wetzlar, Germany). The match range was then used to calculate the anomaly quotient (AQ), which was used as the diagnostic criterion with an AQ of less than 0.7 indicating protanomalous, an AQ range of 0.7 to 1.4 color normal, and an AQ of greater than 1.4 deuteranomalous, where 1 is an equal mixture of red and green, less than 1 is a higher proportion of red, and greater than 1 is a higher proportion of green. Dichromats are able to match the orange test field to almost any red-green mixture by adjusting the brightness, and are thus easily differentiable from AT observers.

Participants

A total of 7 anomalous trichromats (AT) were recruited from The University of Nevada-Reno and the community (3 deuteranomalous, 4 protanomalous, all male), ages 19-42. Color-normal control participants were all UNR students (including author KT), ages 24-38, 2 female. We also tested one dichromat (a protanope) as a further control (see SI Figure 3). 3 AT participants and 5 controls

participated in both Experiment 1 and 2. Chromatic contrast detection thresholds were collected for 6 of the controls and 5 AT participants, 2 AT and 1 CN were not tested because they were not available. All procedures were approved by the University of Nevada, Reno's institutional review board, and all participants provided informed consent prior to testing.

Stimuli

Stimuli were presented on calibrated computer screens in testing rooms at UNR or the fMRI facility at Renown Health Hospital (Reno, NV). Thresholds were collected using a SONY 20SE monitor, with displays controlled by a Cambridge Research Systems (Kent, UK) Visual Stimulus Generator (VSG) board, which allowed for high color resolution. fMRI stimuli were displayed on a 32 in. SensaVue (85 Hz refresh rate) monitor (Invivo, Inc. Gainesville, FL) situated behind the scanner bore and viewed through a head-mounted mirror. The monitor's maximum visual field was 31 deg. by 19 deg. Both monitors were calibrated with a Photo Research (Syracuse, NY) PR655 spectroradiometer, and gun outputs were linearized through lookup tables.

Participants were presented with phase reversing (1 Hz) radial sinewave gratings (0.28 c/deg., 14.5 deg field) defined by chromatic variations along either the L vs M or S vs LM cone-opponent axes (Figure 2). The same stimuli were used in the scanner and during the threshold task, similar to stimuli used by Mullen et al. [31]. Each chromatic direction was shown at 4 levels of chromatic contrast for a total of 8 conditions (Figure 14). Contrasts were scaled roughly as multiples of detection threshold for normal trichromats based on a previous study [67, 68]. In units of pooled cone contrast the highest contrast stimuli were 12% and 70% for L vs M and S vs LM gratings respectively. All stimuli were produced with the Psychophysics Toolbox [69] for MATLAB (Mathworks Inc., Natick, MA).

Psychophysical Isoluminance Determination and Threshold Procedure

Participants were first adapted to a neutral gray background for 1 minute, and then completed a minimum motion task to determine isoluminance [70]. The minimum motion stimuli consisted of alternating achromatic and chromatic concentric sinusoidal gratings that were offset in phase. Participants were instructed to adjust the gratings until the stimuli no longer appeared to radiate inward or outward. Stimulus luminance was adjusted individually for each observer. Individual isoluminance measures were gathered prior to every experimental session.

We then used a temporal 2-alternative forced choice task to measure contrast detection thresholds. The grating was shown in one of two temporal intervals (1 sec. on, 1 sec. off) signaled by beeps, and participants pressed a button to indicate at which interval the grating appeared. Contrast was varied in two randomly interleaved staircases (2 up, 1 down). Each staircase terminated after 10 reversals. The average of the last 8 reversals across each staircase was taken as the participant's detection threshold. S vs LM and L vs M contrast thresholds were collected during the same

session, but across different runs. Thresholds were collected in a separate session and location from the fMRI data.

fMRI Procedure

Data were acquired on a Philips 3T Ingenia scanner using a 32-channel digital SENSE head coil (Philips Medical Systems, Best, Netherlands). Functional data for Experiments 1 and 2 were obtained using T2*-weighted, echo planar images (2 sec. TR, 180 volumes, voxel size 2.75 x 2.75 x 3 $mm^{3,}$ 36 slices, 55 ms inter slice time, 0 mm gaps). We used a block design where a run consisted of 16 blocks of 14 sec. each, interleaved with 8 sec. fixation-only gaps. Each stimulus type was presented twice per run, and the order was counterbalanced across runs. Each run lasted 360 sec. In Experiment 1, all participants completed 8 runs. In Experiment 2, participants completed 6 runs, reduced from Experiment 1. Anatomical scans occurred halfway through a session in order to reduce motion artifacts. Anatomical scans were collected using T1 weighted images (voxel size of 1x1x1 $mm^{3,}$ 30 sec transverse slices, 17 ms TE, 76° flip angle, and 220 x 220 mm^2 field of view). Anatomical and functional runs were collected within a single session for 12 of the participants, while the remaining 2 participants completed functional runs across two sessions.

Fixation Tasks

During scans in Experiment 1, participants completed a simple fixation task to ensure that they were responsive and fixating during the stimulus presentation. The black fixation circle flickered at random, jittered intervals, and the participants were instructed to make a response when a change occurred. In order to further test and control for attentional effects on the BOLD contrast response, Experiment 2 used a more demanding fixation task [41]. The fixation mark for this task was a number that randomly switched from black to white at a jittered rate, while also changing to a random number from 1 to 9. Participants were assigned a random pair of number conjunctions and asked to press a button when either conjunction appeared (e.g. black nine or white three) [43].

fMRI Data Analysis

Images acquired from the scanner were pre-processed before analysis. This included slice scan time correction as well as motion correction, which were both conducted using SPM12 (SPM software package, Wellcome Department, London, UK; http://www.fil.ion.ucl.ac.uk/spm/) and custom lab scripts. Data were motion corrected using a rigid body transform and 7th degree B-spline interpolation. Images were slice scan time corrected (ascending, interleaved) using the first image as the reference slice and resliced into the space of the first image.

Volumetric segmentation of white matter was performed using Freesurfer (v6.0) (http://surfer.nmr.mgh.harvard.edu/) [71, 72]. 3D surface reconstructions of the left and right hemisphere were generated using mrMesh (a function within the mrVista Toolbox) by growing a 3-voxel thick layer above the gray/white boundary. To improve data visualization (i.e. when

projecting functional data onto surfaces), these surfaces were also computationally-inflated using the "smoothMesh" option in mrMesh (8 iterations). Note that the cortical surface models were only used for data visualization and region-of-interest (ROI) definition. All analyses and statistics were performed using the volumetric data.

An anatomical template of retinotopic maps in early visual areas was used to approximate the cortical location of visual areas (V1, V2, V3) and eccentricity ranges that the stimulus subtended (0.00°–9.50°) [73, 74]. The retinotopy template was fitted to each subject's anatomical segmentation using Freesurfer (v6.0) (http://surfer.nmr.mgh.harvard.edu/) [71, 72]. See Figure 4a for an example of the retinotopic template aligned to a subject's cortical surface, and Figure 4b for plots of percent signal change from ROIs drawn from the template. Each ROI showed reliable signal change in response to each color/contrast condition used in the present study.

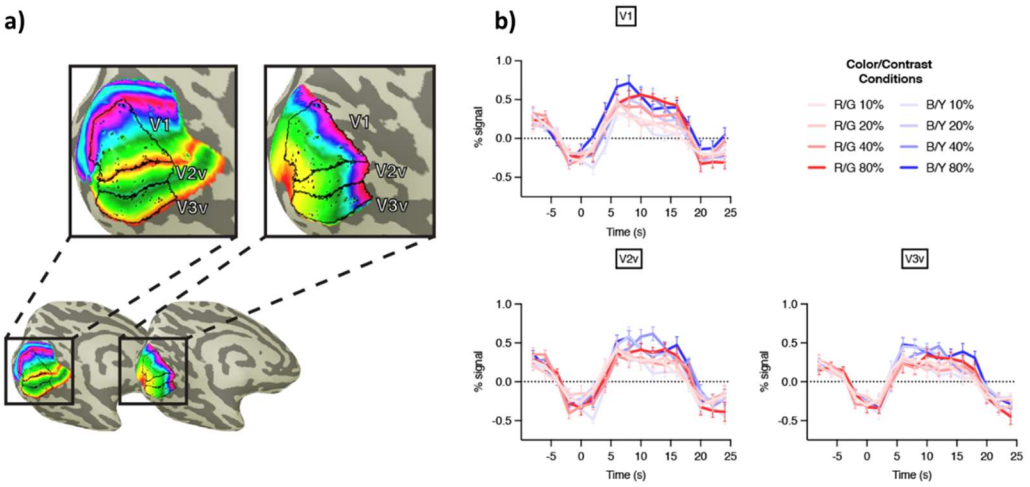

Figure 4. a) Example retinotopic template (polar angle–left, eccentricity—right) aligned to an exemplar subject's left hemisphere (sub-04, CN, exp-02). V1, V2v, and V3v ROIs are drawn on the inflated cortical surface depicted here. The range of the eccentricity map was clipped to 0.00° to 9.50°, corresponding to the range the stimulus subtended. The ROIs have the central 0.00°–0.95° clipped to exclude the fixation point and the mean luminance gray gap between the fixation point and the stimulus. b) Plots of percent signal change in V1, V2v, and V3v in an exemplar subject (sub-04, CN, exp-02). The data was averaged across 6 runs. Each run consisted of 16 blocks where each condition was presented twice (6 runs x 2 repetitions = 12 repetitions total for each condition). The stimulus was presented for 14 seconds (stimulus onset is at 0 seconds in the plots above). A mean luminance blank screen was presented for 8 seconds between blocks.

Fitting Contrast Response Function

Further analysis in the mrVista Toolbox included a general linear model (GLM) of responses across early visual areas (V1, V2v, V3v) for each individual subject. The eccentricity range 0.00°–0.95° was excluded from each ROI prior to analysis to exclude the fixation point and mean luminance gray gap between the fixation point and the stimulus. A standard gamma-function HRF

was used to model the hemodynamic response function [44]. All runs were concatenated and the null gray background condition was used as baseline. After β weights were calculated, a repeated measures ANOVA was performed on these values in order to determine the effects of each condition individually across visual areas.

We then fit data with a contrast response function:

$$R(c) = R_{max} * \frac{c^{(p+q)}}{\left(c^q + c_{50}^q\right)}$$

where rMax, c50, p, and q varied freely, though to aid fitting we set an upper-bound of 4 for p and q since previous work estimates their values for early visual areas to sit between 0.1 and 2.0 [44]. No bounds were set on RMax and c50.

To compute predictions of the reduction model, we scaled the contrast by the ratio of thresholds of CN and AT observers, t:

$$R(c) = R_{max} * \frac{(t * c)^{(p+q)}}{\left((t * c)^q + c_{50}^q\right)}$$

Other values were fixed at values that best fit the mean response from CN observers.

To compute the amount of amplification, we further scaled contrast by a scaling factor, sc, and again kept all other parameters fixed at values from the mean CN response:

$$R(c) = R_{max} * \frac{(sc * t * c)^{(p+q)}}{\left((sc * t * c)^q + c_{50}^q\right)}$$

We estimated sc for each individual AT observer. Because it is a multiplicative factor, we used the log of the scaling parameter in a one-sample t-test to determine if the AT responses were amplified, i.e. they differed significantly from their threshold-scaled predictions, which will be the case if the scaling factor differs from 1.

Acknowledgments

Supported by EY-10834 and P20-GM103650 (MW)

References

1. Neitz, M. and J. Neitz, *Molecular genetics of color vision and color vision defects.* Archives of Ophthalmology, 2000. **118**(5): p. 691-700.
2. MacLeod, D.I. and M. Hayhoe, *Three pigments in normal and anomalous color vision.* JOSA, 1974. **64**(1): p. 92-96.
3. Neitz, J. and M. Neitz, *The genetics of normal and defective color vision.* Vision research, 2011. **51**(7): p. 633-651.
4. Merbs, S.L. and J. Nathans, *Absorption spectra of human cone pigments.* Nature, 1992. **356**(6368): p. 433.
5. Merbs, S.L. and J. Nathans, *Absorption spectra of the hybrid pigments responsible for anomalous color vision.* Science, 1992. **258**(5081): p. 464-467.

6. Nathans, J., et al., *Molecular genetics of inherited variation in human color vision.* Science, 1986. **232**(4747): p. 203-210.
7. Asenjo, A.B., J. Rim, and D.D. Oprian, *Molecular determinants of human red/green color discrimination.* Neuron, 1994. **12**(5): p. 1131-1138.
8. Stockman, A., D.I. MacLeod, and N.E. Johnson, *Spectral sensitivities of the human cones.* J Opt Soc Am A Opt Image Sci Vis, 1993. **10**(12): p. 2491-521.
9. Smith, V.C. and J. Pokorny, *Spectral sensitivity of the foveal cone photopigments between 400 and 500 nm.* Vision Res, 1975. **15**(2): p. 161-71.
10. Vienot, F., et al., *What do colour-blind people see?* Nature, 1995. **376**(6536): p. 127-8.
11. Jacobs, G.H., *Photopigments and the dimensionality of animal color vision.* Neurosci Biobehav Rev, 2018. **86**: p. 108-130.
12. Yaguchi, H., et al., *Computerized simulation of color appearance for anomalous trichromats using the multispectral image.* JOSA A, 2018. **35**(4): p. B278-B286.
13. Webster, M.A., I. Juricevic, and K.C. McDermott, *Simulations of adaptation and color appearance in observers with varying spectral sensitivity.* Ophthalmic Physiol Opt, 2010. **30**(5): p. 602-10.
14. MacLeod, D.I.A., *Colour discrimination, colour constancy, and natural scene statistics (The Verriest Lecture)*, in *Normal and Defective Colour Vision*, J.D. Mollon, J. Pokorny, and K. Knoblauch, Editors. 2003, Oxford University Press: London.
15. Deeb, S., et al., *Genotype-phenotype relationships in human red/green color-vision defects: molecular and psychophysical studies.* American journal of human genetics, 1992. **51**(4): p. 687.
16. Sanocki, E., D.Y. Teller, and S.S. Deeb, *Rayleigh match ranges of red/green color-deficient observers: psychophysical and molecular studies.* Vision research, 1997. **37**(14): p. 1897-1907.
17. Crognale, M., et al., *Severity of color vision defects: electroretinographic (ERG), molecular and behavioral studies.* Vision Research, 1998. **38**(21): p. 3377-3385.
18. Shevell, S., et al., *Relating color discrimination to photopigment genes in deutan observers.* Vision research, 1998. **38**(21): p. 3371-3376.
19. Neitz, J., M. Neitz, and P.M. Kainz, *Visual Pigment Gene Structure and the Severity of Color Vision Defects*. 1996: Science. p. 801-804.
20. Paramei, G.V., *Color space of normally sighted and color-deficient observers reconstructed from color naming.* Psychological Science, 1996. **7**(5): p. 311-317.
21. Bosten, J., *The known unknowns of anomalous trichromacy.* Current Opinion in Behavioral Sciences, 2019. **30**: p. 228-237.
22. Boehm, A.E., D.I. MacLeod, and J.M. Bosten, *Compensation for red-green contrast loss in anomalous trichromats.* J Vis, 2014. **14**(13).
23. Regan, B.C. and J.D. Mollon, *The relative salience of the cardinal axes of colour space in normal and anomalous trichromats* in *Colour Vision Deficiencies* C.R. Cavonius, Editor. 1997, Dordrecht: Kluwer. p. 261-270.
24. Knoblauch, K., B. Marsh-Armstrong, and J.S. Werner, *Suprathreshold contrast response in normal and anomalous trichromats.* J Opt Soc Am A Opt Image Sci Vis, 2020. **37**(4): p. A133-A144.
25. Rabin, J., A. Kryder, and D. Lam, *Binocular facilitation of cone-specific visual evoked potentials in colour deficiency.* Clin Exp Optom, 2018. **101**(1): p. 69-72.
26. Mullen, K.T., D.H. Chang, and R.F. Hess, *The selectivity of responses to red-green colour and achromatic contrast in the human visual cortex: an fMRI adaptation study.* European Journal of Neuroscience, 2015. **42**(11): p. 2923-2933.
27. Johnson, E.N. and K.T. Mullen, *Color in the Cortex*, in *Human Color Vision*. 2016, Springer. p. 189-217.
28. Kuriki, I., et al., *Hue selectivity in human visual cortex revealed by functional magnetic resonance imaging.* Cerebral Cortex, 2015: p. bhv198.

29. Engel, S., X. Zhang, and B. Wandell, *Colour tuning in human visual cortex measured with functional magnetic resonance imaging.* Nature, 1997. **388**(6637): p. 68-71.
30. Wade, A., et al., *fMRI measurements of color in macaque and human.* Journal of Vision, 2008. **8**(10): p. 6.
31. Mullen, K.T., et al., *Selectivity of human retinotopic visual cortex to S-cone-opponent, L/M-cone-opponent and achromatic stimulation.* European Journal of Neuroscience, 2007. **25**(2): p. 491-502.
32. Brouwer, G.J. and D.J. Heeger, *Decoding and reconstructing color from responses in human visual cortex.* J Neurosci, 2009. **29**(44): p. 13992-4003.
33. Brouwer, G.J. and D.J. Heeger, *Categorical clustering of the neural representation of color.* J Neurosci, 2013. **33**(39): p. 15454-65.
34. Persichetti, A.S., et al., *Functional magnetic resonance imaging adaptation reveals a noncategorical representation of hue in early visual cortex.* J Vis, 2015. **15**(6): p. 18.
35. Kim, I., et al., *Neural representations of perceptual color experience in the human ventral visual pathway.* Proceedings of the National Academy of Sciences, 2020. **117**(23): p. 13145-13150.
36. Webster, M.A. and J.D. Mollon, *Adaptation and the color statistics of natural images.* Vision Research, 1997. **37**(23): p. 3283-3298.
37. Engel, S.A. and C.S. Furmanski, *Selective adaptation to color contrast in human primary visual cortex.* Journal of Neuroscience, 2001. **21**(11): p. 3949-3954.
38. Kohn, A., *Visual adaptation: physiology, mechanisms, and functional benefits.* Journal of neurophysiology, 2007. **97**(5): p. 3155-3164.
39. Webster, M.A., *Visual adaptation.* Annual Review of Vision Science, 2015. **1**: p. 547-567.
40. Brewer, A.A., et al., *Visual field maps and stimulus selectivity in human ventral occipital cortex.* Nature neuroscience, 2005. **8**(8): p. 1102-1109.
41. Kay, K.N. and J.D. Yeatman, *Bottom-up and top-down computations in word-and face-selective cortex.* eLife, 2017. **6**: p. e22341.
42. Gandhi, S.P., D.J. Heeger, and G.M. Boynton, *Spatial attention affects brain activity in human primary visual cortex.* Proceedings of the National Academy of Sciences, 1999. **96**(6): p. 3314-3319.
43. Goddard, E., et al., *Combination of subcortical color channels in human visual cortex.* Journal of vision, 2010. **10**(5): p. 25.
44. Boynton, G.M., et al., *Neuronal basis of contrast discrimination.* Vision research, 1999. **39**(2): p. 257-269.
45. Rieke, F. and M.E. Rudd, *The challenges natural images pose for visual adaptation.* Neuron, 2009. **64**(5): p. 605-16.
46. Georgeson, M.A. and G.D. Sullivan, *Contrast constancy: deblurring in human vision by spatial frequency channels.* J Physiol, 1975. **252**(3): p. 627-56.
47. Sincich, L.C. and J.C. Horton, *The circuitry of V1 and V2: integration of color, form, and motion.* Annu. Rev. Neurosci., 2005. **28**: p. 303-326.
48. Solomon, S.G., et al., *Profound contrast adaptation early in the visual pathway.* Neuron, 2004. **42**(1): p. 155-62.
49. Chang, D.H.F., R.F. Hess, and K.T. Mullen, *Color responses and their adaptation in human superior colliculus and lateral geniculate nucleus.* Neuroimage, 2016. **138**: p. 211-220.
50. Gollisch, T. and M. Meister, *Eye smarter than scientists believed: neural computations in circuits of the retina.* Neuron, 2010. **65**(2): p. 150-64.
51. Kohn, A., *Visual adaptation: physiology, mechanisms, and functional benefits.* J Neurophysiol, 2007. **97**(5): p. 3155-64.
52. Lutze, M., J. Pokorny, and V.C. Smith, *Achromatic parvocellular contrast gain in normal and color defective observers: Implications for the evolution of color vision.* Vis Neurosci, 2006. **23**(3-4): p. 611-6.

53. Conway, B.R., *Color signals through dorsal and ventral visual pathways.* Vis Neurosci, 2014. **31**(2): p. 197-209.
54. Zaidi, Q. and B. Conway, *Steps towards neural decoding of colors.* Current Opinion in Behavioral Sciences, 2019. **30**: p. 169-177.
55. Kim, I., et al., *Neural representations of perceptual color experience in the human ventral visual pathway.* Proc Natl Acad Sci U S A, 2020. **117**(23): p. 13145-13150.
56. Tregillus, K.E. and S.A. Engel, *Long-term adaptation to color.* Current Opinion in Behavioral Sciences, 2019. **30**: p. 116-121.
57. Werner, J.S., B. Marsh-Armstrong, and K. Knoblauch, *Adaptive changes in color vision from long-term filter usage in anomalous but not normal trichromacy.* Current Biology, 2020.
58. Webster, M.A., *Human colour perception and its adaptation.* Network: Computation in Neural Systems, 1996. **7**: p. 587-634.
59. Rieke, F. and M.E. Rudd, *The challenges natural images pose for visual adaptation.* Neuron, 2009. **64**(5): p. 605-616.
60. von der Twer, T. and D.I. MacLeod, *Optimal nonlinear codes for the perception of natural colours.* Network: Computation in Neural Systems, 2001. **12**(3): p. 395-407.
61. Haak, K.V., et al., *Four days of visual contrast deprivation reveals limits of neuronal adaptation.* Current Biology, 2014. **24**(21): p. 2575-2579.
62. Kwon, M., et al., *Adaptive changes in visual cortex following prolonged contrast reduction.* Journal of vision, 2009. **9**(2): p. 20.
63. Zhang, P., et al., *Effects of orientation-specific visual deprivation induced with altered reality.* Current Biology, 2009. **19**(22): p. 1956-1960.
64. Clifford, C.W., et al., *Visual adaptation: neural, psychological and computational aspects.* Vision Research, 2007. **47**(25): p. 3125-31.
65. Solomon, S.G. and A. Kohn, *Moving sensory adaptation beyond suppressive effects in single neurons. , .* Current Biology, 2014. **24**(20): p. R1012-R1022.
66. Neitz, M. and J. Neitz, *Curing color blindness—mice and nonhuman primates.* Cold Spring Harb Perspect Med, 2014. **4:a017418**.
67. Webster, M.A. and J.D. Mollon, *The influence of contrast adaptation on color appearance.* Vision Research, 1994. **34**(15): p. 1993-2020.
68. Webster, M.A., et al., *Variations in normal color vision. I. Cone-opponent axes.* JOSA A, 2000. **17**(9): p. 1535-1544.
69. Brainard, D.H., *The psychophysics toolbox.* Spatial vision, 1997. **10**: p. 433-436.
70. Cavanagh, P., D.I. MacLeod, and S.M. Anstis, *Equiluminance: spatial and temporal factors and the contribution of blue-sensitive cones.* J Opt Soc Am A, 1987. **4**(8): p. 1428-38.
71. Fischl, B., et al., *High-resolution intersubject averaging and a coordinate system for the cortical surface.* Human brain mapping, 1999. **8**(4): p. 272-284.
72. Fischl, B. and A.M. Dale, *Measuring the thickness of the human cerebral cortex from magnetic resonance images.* Proceedings of the National Academy of Sciences, 2000. **97**(20): p. 11050-11055.
73. Benson, N.C., et al., *The retinotopic organization of striate cortex is well predicted by surface topology.* Current Biology, 2012. **22**(21): p. 2081-2085.
74. Benson, N.C., et al., *Correction of distortion in flattened representations of the cortical surface allows prediction of V1-V3 functional organization from anatomy.* PLoS Comput Biol, 2014. **10**(3): p. e1003538.
75. Cohen, J.P., *Statistical Power Analysis for the Behavioral Sciences*. 2nd ed. 1988, New York, NY: Routledge Academic.

Supplemental Information

Statistics: Experiment 1 (V1, V2v, V3v Mixed ANOVA)

A:2 x (3 x 2 x 4) mixed ANOVA was conducted on the β weights calculated from the GLM analysis of the fMRI data (N = 10: 5 CN and 5 AT). The between subject factor was *Color Vision Type* (CN, AT), and the three within subject factors were *Visual Area* (V1, V2v, V3v), *Color* (R/G, B/Y), and *Contrast* (10%, 20%, 40%, 80%). See SI Table 1 for a summary of ANOVA main effects and interactions. The between subject effect *Color Vision Type* was not significant ($F_{1,8} = 0.426$, $p = 0.532$, $\eta_p^2 = 0.051$). The effect size reported for this between-subject effect (as indicated by η_p^2) is considered small as per the effect size conventions of [75]. The main effects *Visual Area* ($F_{1.750,14.002} = 10.347$, $p = 0.002$, $\eta_p^2 = 0.564$), *Color* ($F_{1,8} = 21.950$, $p = 0.002$, $\eta_p^2 = 0.733$), and *Contrast* ($F_{2.520,20.158} = 19.453$, $p < 0.001$, $\eta_p^2 = 0.709$) were significant. In terms of interactions, the *Color x Contrast* interaction was significant ($F_{3.296,26.365} = 3.433$, $p = 0.028$, $\eta_p^2 = 0.300$) as well as the *Visual Area x Color x Contrast* interaction ($F_{2.398,19.181} = 5.681$, $p = 0.009$, $\eta_p^2 = 0.415$). In terms of interactions involving the between subject-effect *Color Vision Type*, the *Color x Color Vision Type* interaction was significant ($F_{1,8} = 11.079$, $p = 0.010$, $\eta_p^2 = 0.581$). The *Color x Contrast x Color Vision Type* interaction was also significant ($F_{3.296,26.365} = 3.887$, $p = 0.018$, $\eta_p^2 = 0.327$).

The effect sizes reported here for the within-subject effects and interactions (as indicated by η_p^2) are considered large as per the effect size conventions of [75]. All statistics reported in this section were Greenhouse-Geisser corrected.

SI - Table 1
Summary of ANOVA main effects and interactions for Experiment 1.

	df	Error	F	p	η_p^2	Power
Visual Area	**1.750**	**14.002**	**10.347**	**0.002**	**0.564**	**0.947**
Visual Area x Color Vision Type	1.750	14.002	2.341	0.137	0.226	0.373
Color	**1.000**	**8.000**	**21.950**	**0.002**	**0.733**	**0.983**
Color x Color Vision Type	**1.000**	**8.000**	**11.079**	**0.010**	**0.581**	**0.829**
Contrast	**2.520**	**20.158**	**19.453**	**<0.001**	**0.709**	**1.000**
Contrast x Color Vision Type	2.520	20.158	0.956	0.420	0.107	0.209
Visual Area x Color	1.323	10.580	3.486	0.082	0.303	0.444
Visual Area x Color x Color Vision Type	1.323	10.580	2.685	0.126	0.251	0.356
Color x Contrast	**3.296**	**26.365**	**3.433**	**0.028**	**0.300**	**0.731**
Color x Contrast x Color Vision Type	**3.296**	**26.365**	**3.887**	**0.018**	**0.327**	**0.788**
Visual Area x Color x Contrast	**2.398**	**19.181**	**5.681**	**0.009**	**0.415**	**0.846**
Visual Area x Color x Contrast x Color Vision Type	2.398	19.181	2.410	0.109	0.232	0.463

Notes: Reported statistics were adjusted using Greenhouse-Geisser correction. Rows in bold represent interactions with p < 0.05.

Statistics: Experiment 2 (V1, V2v, V3v Mixed ANOVA)

The same mixed ANOVA as performed in *Experiment 1* was conducted here (N = 12: 7 CN and 5 AT). See SI Table 2 for a summary of ANOVA main effects and interactions. The between subject effect *Color Vision Type* was not significant ($F_{1,10} = 1.415$, $p = 0.262$, $\eta_p^2 = 0.124$).The effect size reported for this between-subject effect (as indicated by η_p^2) is considered medium as per the effect size conventions of [75]. The main effects *Visual Area* ($F_{1.844,18.443} = 8.563$, $p = 0.003$, $\eta_p^2 = 0.461$), *Color* ($F_{1,10} = 8.246$, $p = 0.017$, $\eta_p^2 = 0.452$), and *Contrast* ($F_{1.980,19.804} = 19.905$, $p < 0.001$, $\eta_p^2 = 0.666$) were significant. The interaction *Color x Contrast* was significant ($F_{3.170,31.704} = 8.177$, $p < 0.001$, $\eta_p^2 = 0.450$). In terms of interactions involving the between subject effect *Color Vision Type*, the *Visual Area x Color x Color Vision Type* interaction was significant ($F_{1.449,14.491} = 5.909$, $p = 0.020$, $\eta_p^2 = 0.450$).

The effect sizes reported here for the within-subject effects and interactions (as indicated by η_p^2) are considered large as per the effect size conventions of [75]. All statistics reported in this section were Greenhouse-Geisser corrected.

SI – Table 2
Summary of ANOVA main effects and interactions for Experiment 1.

	df	Error	F	p	η_p^2	Power
Visual Area	**1.844**	**18.443**	**8.563**	**0.003**	**0.461**	**0.923**
Visual Area x Color Vision Type	1.844	18.443	0.731	0.484	0.068	0.151
Color	**1.000**	**10.000**	**8.246**	**0.017**	**0.452**	**0.735**
Color x Color Vision Type	1.000	10.000	1.211	0.297	0.108	0.169
Contrast	**1.980**	**19.804**	**19.905**	**<0.001**	**0.666**	**1.000**
Contrast x Color Vision Type	1.980	19.804	0.764	0.478	0.071	0.161
Visual Area x Color	1.449	14.491	0.879	0.403	0.081	0.157
Visual Area x Color x Color Vision Type	**1.449**	**14.491**	**5.909**	**0.020**	**0.371**	**0.715**
Color x Contrast	**3.170**	**31.704**	**8.177**	**<0.001**	**0.450**	**0.987**
Color x Contrast x Color Vision Type	3.170	31.704	2.084	0.119	0.172	0.496
Visual Area x Color x Contrast	2.361	23.611	0.510	0.637	0.049	0.129
Visual Area x Color x Contrast X Color Vision Type	2.361	23.611	0.370	0.729	0.036	0.106

Notes: Reported statistics were adjusted using Greenhouse-Geisser correction. Rows in bold represent interactions with p < 0.05.

Statistics: Experiment 1 vs Experiment 2 (V1, V2v, V3v Mixed ANOVA)

A:2 x (2 x 3 x 2 x 4) mixed ANOVA was conducted on the β weights calculated from the GLM analysis of the fMRI data across Experiments 1 & 2. Only subjects who participated in both experiments were included in this analysis (N = 8: 5 CN and 3 AT). The between subject factor was *Color Vision Type* (CN, AT), and the four within subject factors were *Attention* (Experiment 1 – low attention task, Experiment 2 – high attention task), *Visual Area* (V1, V2v, V3v), *Color* (R/G, B/Y), and *Contrast* (10%, 20%, 40%, 80%). See SI Table 3 for a summary of ANOVA main effects and interactions. The between subject effect *Color Vision Type* was not significant ($F_{1,6}$ =

0.055, $p = 0.822$, $\eta_p^2 = 0.055$). The effect size reported for this between-subject effect (as indicated by η_p^2) is considered small as per the effect size conventions of [75].

The main effect of *Attention* was not significant ($F_{1,6.000} = 3.736$, $p = 0.101$, $\eta_p^2 = 0.384$). No interactions involving the effect of *Attention* such as *Attention x Color x Color Vision Type* ($F_{1,6.000} = 2.651$, $p = 0.155$, $\eta_p^2 = 0.306$) nor *Attention x Color x Contrast* ($F_{2.318,13.910} = 0.728$, $p = 0.520$, $\eta_p^2 = 0.155$) were significant. See SI Table 3 for more detail on the other interactions involving *Attention*. The effect size reported here for *Attention* and the *Attention x Color x Color Vision Type* interaction (as indicated by η_p^2) are considered large as per the effect size conventions of [75]. However, the effect size for the *Attention x Color x Contrast* interaction is considered medium. The main effects *Visual Area* ($F_{1.695,10.172} = 8.718$, $p = 0.0008$, $\eta_p^2 = 0.592$), *Color* ($F_{1,6} = 11.386$, $p = 0.015$, $\eta_p^2 = 0.655$), and *Contrast* ($F_{1.975,11.741} = 25.815$, $p < 0.001$, $\eta_p^2 = 0.811$) were significant. The interaction *Visual Area x Contrast* was also significant ($F_{2.616,15.698} = 4.814$, $p = 0.017$, $\eta_p^2 = 0.445$). In terms of interactions involving the between subject effect *Color Vision Type*, the *Visual Area x Color x Color Vision Type* interaction was significant ($F_{2.616,15.698} = 3.611$, $p = 0.042$, $\eta_p^2 = 0.376$).

The remainder of the effect sizes reported here for the within-subject effects and interactions (as indicated by η_p^2) are considered large as per the effect size conventions of [75]. All statistics reported in this section were Greenhouse-Geisser corrected.

SI - Table 3
Summary of ANOVA main effects and interactions for comparison between the attentional effects of Experiment 1 and Experiment 2.

	df	Error	F	p	η_p^2	Power
Attention	1.000	6.000	3.736	0.101	0.384	0.370
Attention x Color Vision Type	1.000	6.000	0.465	0.521	0.072	0.089
Visual Area	**1.695**	**10.172**	**8.718**	**0.008**	**0.592**	**0.873**
Visual Area x Color Vision Type	1.695	10.172	1.342	0.298	0.183	0.215
Color	**1.000**	**6.000**	**11.386**	**0.015**	**0.655**	**0.802**
Color x Color Vision Type	1.000	6.000	3.854	0.097	0.391	0.379
Contrast	**1.957**	**11.741**	**25.815**	**<0.001**	**0.811**	**1.000**
Contrast x Color Vision Type	1.957	11.741	1.544	0.254	0.205	0.262
Attention x Visual Area	1.736	10.417	4.045	0.054	0.403	0.555
Attention x Visual Area x Color Vision Type	1.736	10.417	2.474	0.136	0.292	0.368
Attention x Color	1.000	6.000	1.495	0.267	0.199	0.179
Attention x Color x Color Vision Type	1.000	6.000	2.651	0.155	0.306	0.280
Visual Area x Color	1.369	8.211	2.963	0.117	0.331	0.370
Visual Area x Color x Color Vision Type	1.369	8.211	4.917	0.049	0.450	0.560
Attention x Visual Area x Color	1.558	9.347	1.361	0.294	0.185	0.208
Attention x Visual Area x Color x Color Vision	1.558	9.347	0.312	0.687	0.049	0.084

Continued…	df	Error	F	p	η_p^2	Power
Attention x Contrast	2.406	14.435	3.629	0.046	0.377	0.619
Attention x Contrast x Color Vision Type	2.406	14.435	0.821	0.480	0.120	0.173
Visual Area x Contrast	**2.616**	**15.698**	**4.814**	**0.017**	**0.445**	**0.780**
Visual Area x Contrast x Color Vision Type	**2.616**	**15.698**	**3.611**	**0.042**	**0.376**	**0.646**
Attention x Visual Area x Contrast	2.770	16.619	0.445	0.709	0.069	0.118
Attention x Visual Area x Contrast x Color Vision Type	2.770	16.619	1.158	0.352	0.162	0.248
Color x Contrast	**2.120**	**12.721**	**4.678**	**0.028**	**0.438**	**0.692**
Color x Contrast x Color Vision Type	2.120	12.721	0.360	0.716	0.057	0.097
Attention x Color x Contrast	2.318	13.910	0.728	0.520	0.108	0.155
Attention x Color x Contrast x Color Vision Type	2.318	13.910	2.280	0.134	0.275	0.410
Visual Area x Color x Contrast	**2.865**	**17.187**	**3.563**	**0.038**	**0.373**	**0.673**
Visual Area x Color x Contrast x Color Vision Type	2.865	17.187	4.965	0.012	0.453	0.824
Attention x Visual Area x Color x Contrast	2.267	13.599	1.878	0.188	0.238	0.339
Attention x Visual Area x Color x Contrast x Color Vision Type	2.267	13.599	1.026	0.394	0.146	0.200

Notes: Reported statistics were adjusted using Greenhouse-Geisser correction. Rows in bold represent interactions with $p < 0.05$.

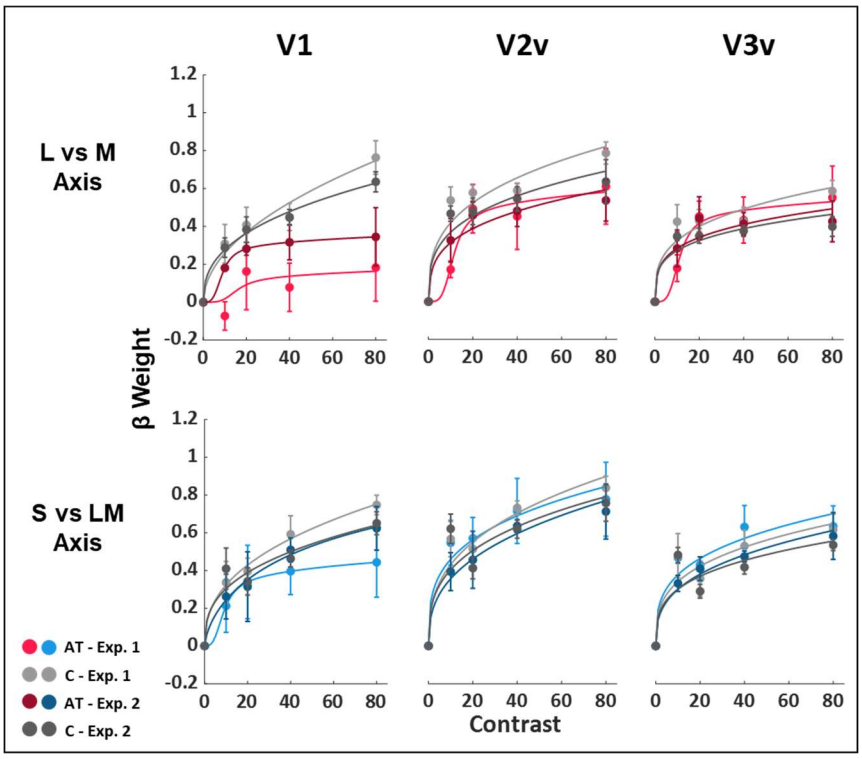

SI - Figure 1. Comparison of Experiment 1 (simple fixation task) and Experiment 2 (high-attention fixation task) showing only data from those who participated in both experiments. ATs are shown in red and blue and CNs are shown in gray. Experiment 1 data shown in lighter colors. Solid lines are fitted CRFs.

Individual Data

Individual data shows that most participants showed the same general pattern with less evidence of compensation in area V1, and increasing compensation in areas V2v and V3v. However, some participants deviated from this pattern. For example, participants DA-04 appears to show consistently higher responses in all three areas.

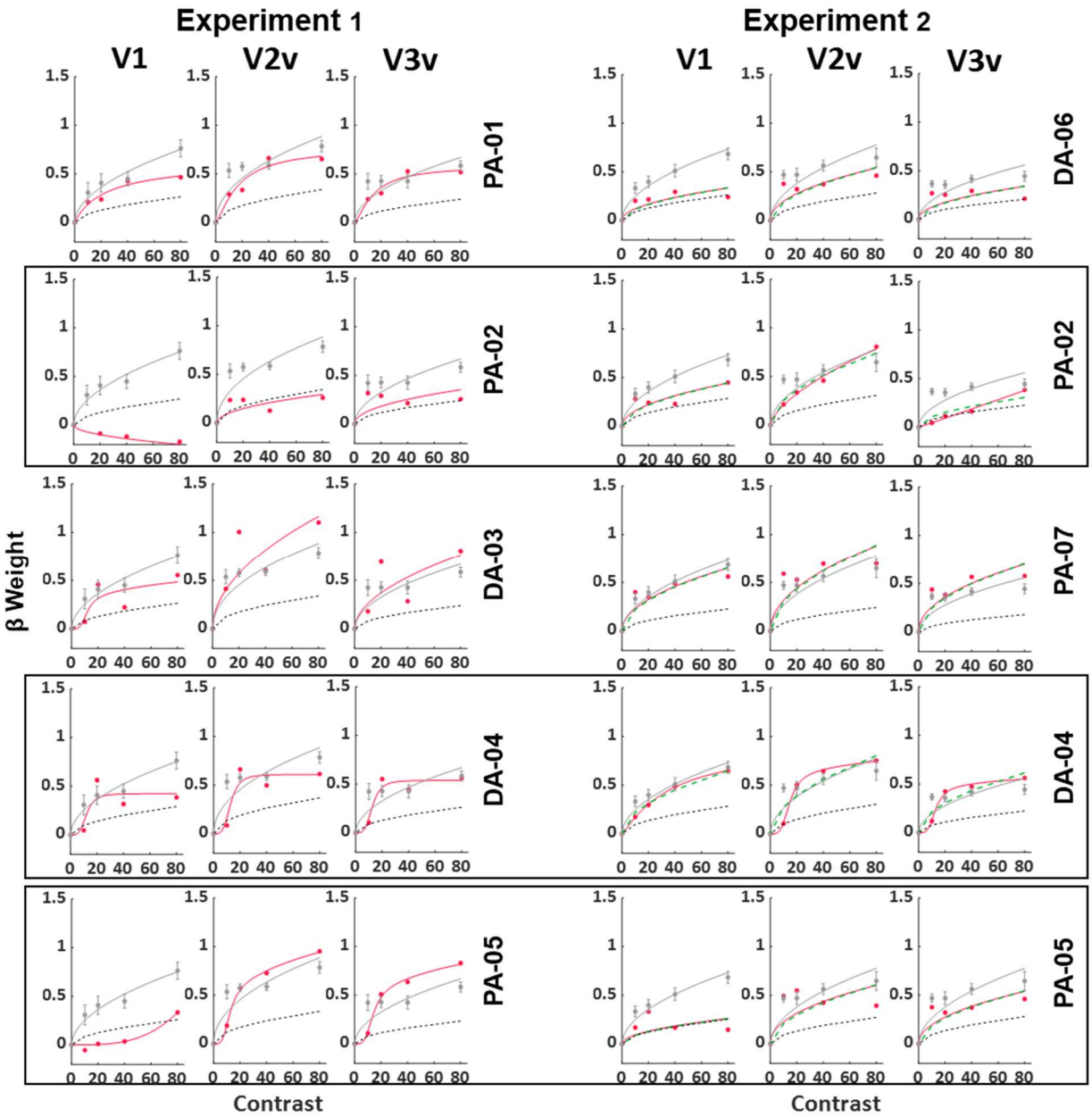

SI – Figure 2. L vs M data responses for each AT observer (red), for Experiment 1 (simple fixation task) and Experiment 2 (high-attention fixation task) plotted alongside the mean CN responses (gray), and the threshold prediction (dashed black line). Participants who were in both experiments are outlined in black. The fitted line with scaling factor is shown in green in the Experiment 2 plots.

Dichromatic Observer

As a further control condition, we also tested one dichromatic (protanopic) participant in the fMRI paradigm of Experiment 2 (male, 31). PN-01's data can be seen in SI Figure 3, where it is compared to the average responses for the anomalous trichromats. This observer's thresholds were 9.14 for the L vs. M stimuli and 2.02 for the S stimuli. These are similar to the thresholds we obtained for the anomalous observers. PN-01 was diagnosed as a protanope based on anomaloscope settings, in which he accepted all red-green ratios as matches. As expected, the L vs. M Bold activation for this dichromatic observer was substantially weaker than for the ATs, yet surprisingly, his S responses were also lower. There were no regions where this participant showed a monotonic contrast response function for the L vs M stimuli, and the magnitude of the response at the highest contrast (80) was no greater than the response to the lowest contrast (10). Thus we were unable to fit a reasonable CRF to his data. This provides evidence that our stimuli were specifically targeting the chromatic responses in the normal and anomalous observers, and thus were not driven simply by potential luminance artifacts in the gratings.

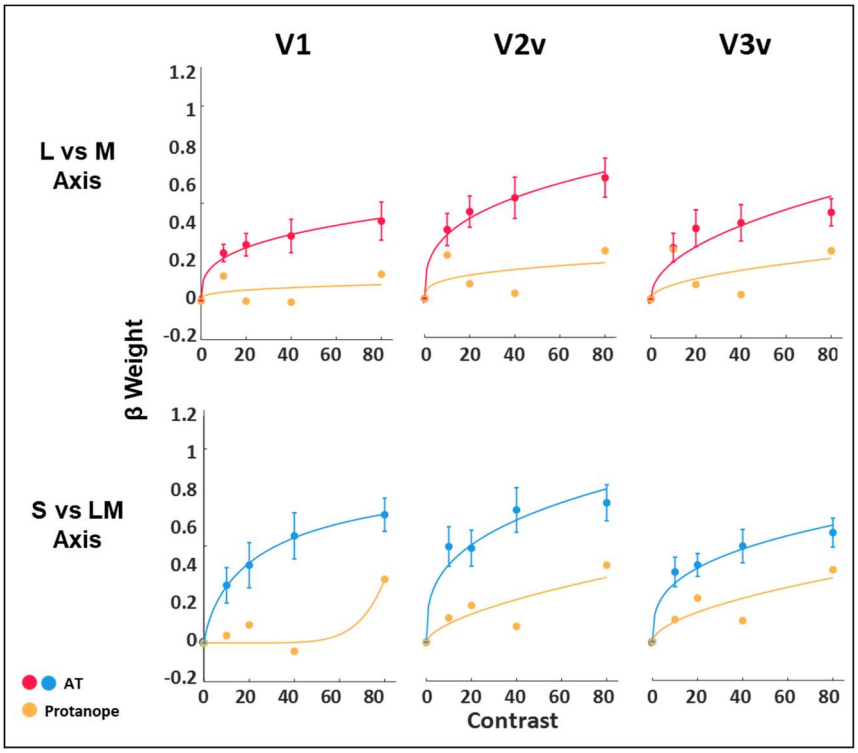

SI - Figure 3. BOLD responses to chromatic contrast levels for one protanopic participant (yellow), compared to the mean activation across AT observers for areas V1, V2v, V3v. L vs M responses are in the top row, and S vs LM responses are in the bottom row.